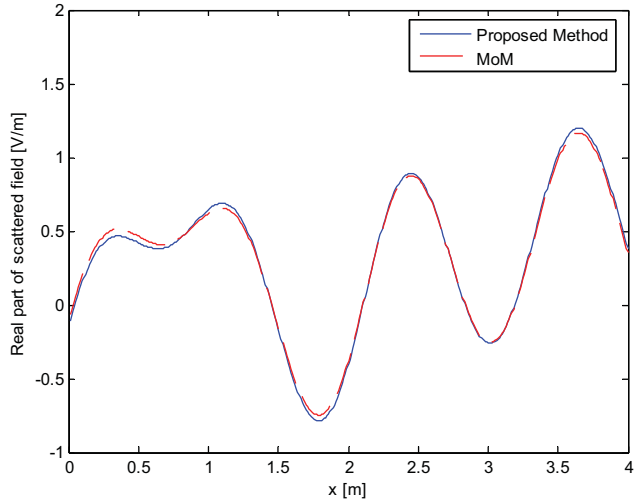

(a)

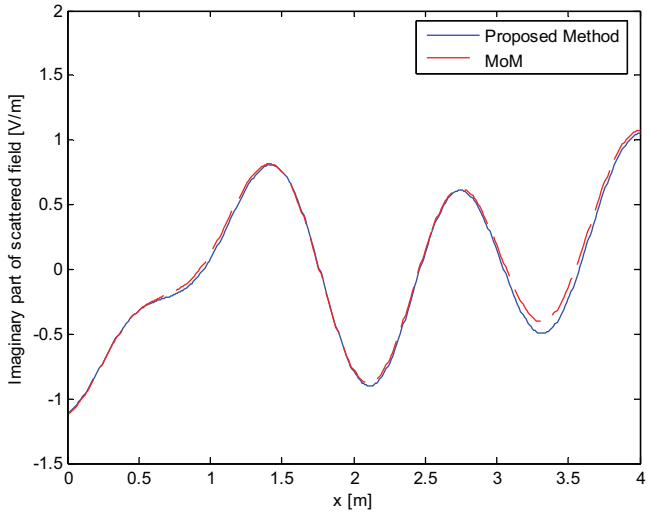

(b)

Figure 4 Scattered field above triangle surface within one period. (a) Real part, (b) Imaginary part ($\phi_0 = 45°$, $y_0 = 3$, $P = 4$, $\alpha = 0.4$, $f(x) = 0.4|x - 2| - 0.4$). [Color figure can be viewed in the online issue, which is available at www.interscience.wiley.com]

REFERENCES

1. K.A. Zaki and A.R. Neureuther, Scattering from a perfectly conducting surface with a sinusoidal height profile-TE polarization, IEEE Trans Antennas Propagat 19 (1971), 208–214.
2. G.M. Whiteman, D.M. Leskiw, and F. Schwering, Rigorous theory of scattering by perfectly conducting periodic surfaces with trapezoidal height profile—TE and TM polarization, J Opt Soc Am 70 (1980), 1495–1503.
3. J.A. Desanto, Scattering from a perfectly reflecting arbitrary periodic surface—An exact theory, Radio Sci 16 (1981), 1315–1326.
4. C. Eftimiu and P.L. Huddleston, Scattering of electromagnetic waves by conducting periodic surfaces —A comparison of exact integral equation methods, Radio Sci 22 (1987), 815–824.
5. L. Tsang, J.A. Kong, K.H. Ding, and C.O. Ao, Scattering of electromagnetic waves: Numerical simulations, Wiley, 2001.
6. A. Lakhtakia, V.K. Varadan, and V.V. Varadan, A T-matrix approach for EM scattering by a perfectly conducting periodic surface, Proc IEEE 73 (1985), 1238–1239.
7. G.S. Wallinga, E.J. Rothwell, K.M. Chen, and D.P. Nyquist, Efficient computation of the two-dimensional periodic Green's function, IEEE Trans Antennas Propagat 47 (1999), 895–897.
8. N.S. Tezel and S. Paker, Electromagnetic scattering from cylinder described by high-order inhomogeneous impedance boundary conditions, Microwave Opt Technol Lett 48 (2006), 1148–1151.
9. J.A. Kong, Electromagnetic wave theory, 2nd ed., Wiley, New York, 1990.

WIDEBAND INTEGRATED MONOPOLE SLOT ANTENNA FOR WLAN/WiMAX OPERATION IN THE MOBILE PHONE

Kin-Lu Wong and Peng-Yu Lai
Department of Electrical Engineering, National Sun Yat-Sen University, Kaohsiung 804, Taiwan; Corresponding author: laipy@ema.ee.nsysu.edu.tw

Received 9 December 2007

ABSTRACT: *A promising design of the wideband integrated monopole slot antenna for WLAN/WiMAX operation in the mobile phone is presented. The antenna is integrated at one corner of the system circuit board of the mobile phone and consists of two portions, one on-board slotted portion and one add-on portion. The add-on portion is printed on a small FR4 substrate as a surface-mount element, which is vertically mounted and connected to the on-board slotted portion to form as a monopole slot antenna. This integrated monopole slot antenna occupies a small volume in the mobile phone and shows a very wide bandwidth covering WLAN operation in the 2400–2484 MHz band and WiMAX operation in the 2500–2690/3300–3700 MHz bands. Detailed results of impedance and radiation characteristics of the proposed antenna are presented and discussed.* © 2008 Wiley Periodicals, Inc.
Microwave Opt Technol Lett 50: 2000–2005, 2008; Published online in Wiley InterScience (www.interscience.wiley.com). DOI 10.1002/mop.23566

Key words: *monopole slot antennas; WLAN antennas; WiMAX antennas; integrated antennas; mobile phone antennas*

1. INTRODUCTION

Nowadays, the wireless local area network (WLAN) system and the worldwide interoperability for microwave access (WiMAX) system [1] are very popular techniques for wireless Internet access. With the complementary capability between WLAN and WiMAX systems, seamless internet access for mobile users becomes possible. To cover WLAN and WiMAX operation [2–5], however, a wide operating band for the employed antenna in portable mobile devices is required. For this application, it has been demonstrated that the monopole slot or open slot antenna is very promising in providing a wide operating band with a compact antenna size [6–12]. The monopole slot antenna is operated as a quarter-wavelength resonant structure and is different from the conventional slot antenna resonating at a half-wavelength [13–16]. Hence, the monopole slot antenna can have a compact size for a fixed operating frequency, which makes it very attractive for application in the mobile devices. For the monopole slot antennas that have been reported, however, they are all printed on the system circuit board of the mobile devices. In this case, the monopole slot antenna still occupies some valuable spaces on the system circuit board, although it has a smaller required size than the conventional slot antenna.

In this article, we present a novel integrated monopole slot antenna for WLAN operation in the 2.4 GHz band (2400–2484 MHz) and WiMAX operation in the 2.5/3.5 GHz bands (2500–

2690/3300–3700 MHz) in the mobile phone. The antenna comprises one on-board slotted portion and one add-on (surface-mount) portion. Owing to the use of the add-on portion, which is to be surface-mounted to the system circuit board of the mobile phone and then integrated to the on-board slotted portion on the system circuit board, the proposed monopole slot antenna will occupy a much smaller area on the system circuit board than the conventional monopole slot antenna. Although a much smaller board space is occupied, the proposed antenna can provide a wide operating band of about 1.8 GHz (from about 2.2 to 4.0 GHz, 58% in 10-dB return-loss bandwidth) to cover the desired WLAN/WiMAX operation. Detailed design considerations of the antenna are described in the article, and the antenna was fabricated and studied. Obtained results of the fabricated antenna are presented and discussed.

2. ANTENNA DESIGN

Figure 1 shows the proposed monopole slot antenna for WLAN/WiMAX operation in the mobile phone. The monopole slot antenna is formed by one on-board slotted portion located at one corner of the system circuit board of the mobile phone and one add-on portion as a surface-mount element. The system circuit board in the study is a 0.8-mm thick FR4 substrate of length 100 mm and width 40 mm. The on-board slotted portion is located at one corner of the top edge of the circuit board as shown in the figure. The slotted portion has a main slot of length 13 mm (a) and width 3 mm (t) and a triangular end slot of angle 45° (α). With the presence of the triangular end slot, good impedance matching for frequencies over the operating band of the antenna can be much easier to achieve.

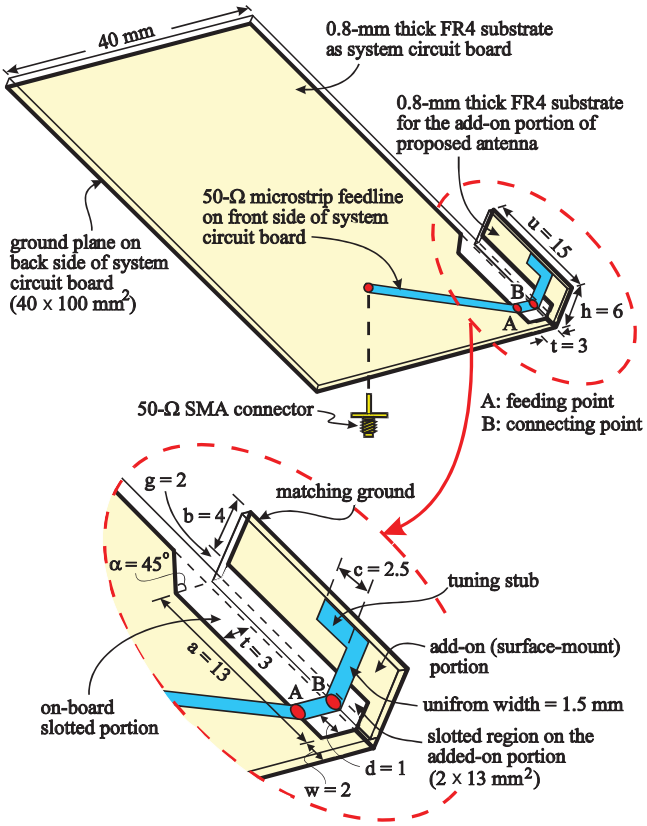

Figure 1 Configuration of the wideband integrated monopole slot antenna for WLAN/WiMAX operation in the mobile phone. [Color figure can be viewed in the online issue, which is available at www.interscience.wiley.com]

The add-on portion is printed on a small 0.8-mm thick FR4 substrate of length 15 mm (u) and width 6 mm (h). Note that in order for the proposed antenna to be promising for thin mobile phone applications, the height h of the add-on portion is selected to be 6 mm only. On the back side of the add-on portion there is mainly a printed matching ground of length 15 mm (u) and width 4 mm (b) and a slotted region of length 13 mm ($u - w$) and width 2 mm (g); the parameter w is the width (2 mm here) of the connecting strip to be connected to the system ground plane printed on the back side of the circuit board. On the front side of the add-on portion, an inverted-L tuning stub is printed. By varying the length c of the open-end section of the tuning stub, impedance matching for frequencies over the operating band of the antenna can be adjusted. The add-on portion is to be surface-mounted to the circuit board and connected to the on-board slotted portion at point B shown in the figure and to the system ground plane through the narrow conducting strip on the add-on portion. With the add-on portion integrated to the on-board slotted portion, the proposed monopole slot antenna with a slot width 5 mm ($t + g$) and length 13 mm (a) is formed. To excite the monopole slot antenna, a 50-Ω microstrip feedline printed on the front side of the circuit board is used. The feeding point is at point A, and the location of the feedline is 1 mm (d) to the shorted end of the monopole slot in this design.

The selection of the slot length 13 mm (a) in the proposed antenna ensures the lower edge frequency of the obtained operating band less than 2.4 GHz. Owing to the presence of the FR4 substrate which decreases the required resonant length, the slot length 13 mm is much smaller than 0.25 wavelength of the frequency at 2.4 GHz. By selecting a larger slot width ($t + g$), the antenna's achievable bandwidth can be increased. For the present slot width of 5 mm ($t + g$), the obtained bandwidth is large enough to cover the 2.4 GHz WLAN operation and 2.5/3.5 GHz WiMAX operation. By varying the lengths c and d, the parameters related to the microstrip feedline, the impedance bandwidth for frequencies over the desired operating band (from 2.4 to 3.7 GHz) can be adjusted. For the parameters α and b, they mainly affect the impedance matching for frequencies in the high-frequency portion of the operating band.

3. RESULTS AND DISCUSSION

The proposed monopole slot antenna with dimensions given in Figure 1 was fabricated and studied. Figure 2 shows the measured and simulated return loss for the fabricated antenna. The simulated results are obtained using Ansoft HFSS (High Frequency Structure Simulator) [17], and good agreement between the measured data and simulated results is seen. From the measured data, a wide operating band defined by 10-dB return loss of about 1.8 GHz (2205–4020 MHz) or 58% centered at 3.1 GHz is obtained. This wide bandwidth easily covers the 2.4 GHz WLAN operation and 2.5/3.5 GHz WiMAX operation.

Figure 3 shows the simulated return loss of the proposed antenna and the reference antenna (a conventional PIFA with corresponding dimensions). The geometry of the reference antenna is also shown in the figure. From the results, it is seen that the obtained bandwidth of the reference antenna is only about 0.7 GHz (from about 3.3 to 4.0 GHz), much smaller than that of the proposed antenna. Also note that the reference antenna is operated as a quarter-wavelength structure [18], and owing to the presence of the FR4 substrate, its resonant length (about 15 mm here) corresponds to about 0.18 wavelength of the center operating frequency 3.7 GHz here.

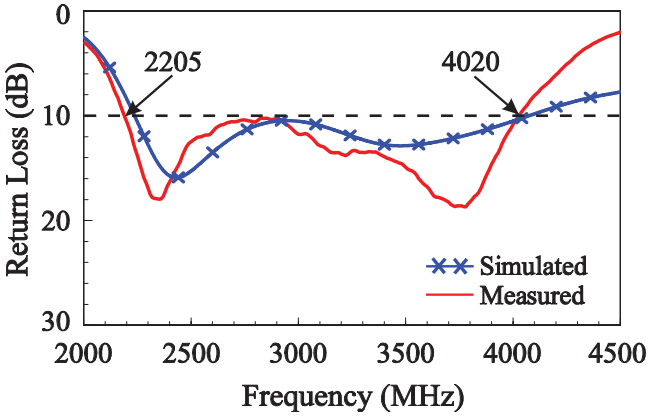

Figure 2 Measured and simulated return loss for the proposed antenna. [Color figure can be viewed in the online issue, which is available at www.interscience.wiley.com]

Figure 4 shows the simulated return loss as a function of the height h and the length w of the proposed antenna. In Figure 4(a), the results for the height h varied from 3 to 5 mm are presented. In this case, the width b of the matching ground is varied, with other dimensions fixed as shown in Figure 1. Results indicate that the matching ground has strong effects on the impedance matching of the high-frequency portion of the antenna's operating band. A larger width of the matching ground can also lead to a decrease in the lower edge frequency of the operating band. The results for the width w varied from 1 to 3 mm are shown in Figure 4(b); the total length u of the antenna is also increased with an increase in w. From the results, it indicates that the width w should be selected to be larger than 2 mm to achieve good impedance matching over the desired operating band.

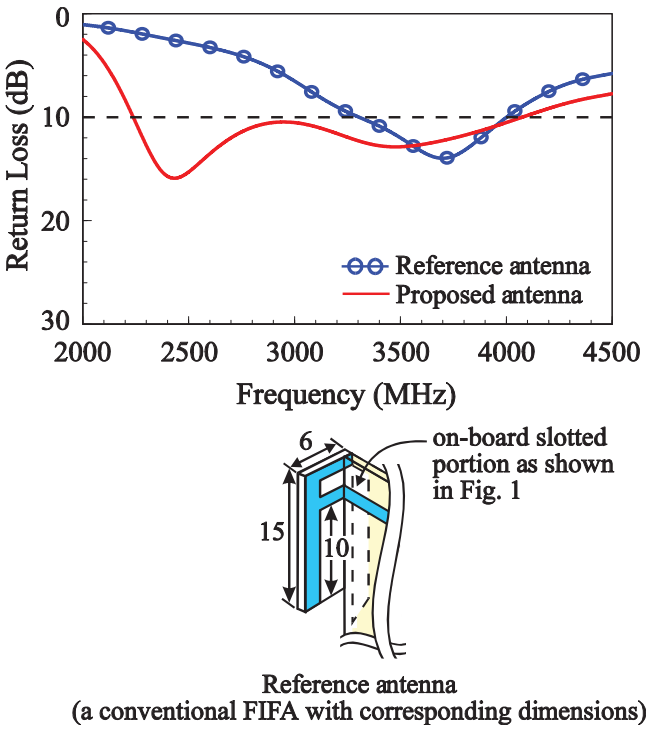

Figure 3 Simulated return loss of the proposed antenna and the reference antenna. [Color figure can be viewed in the online issue, which is available at www.interscience.wiley.com]

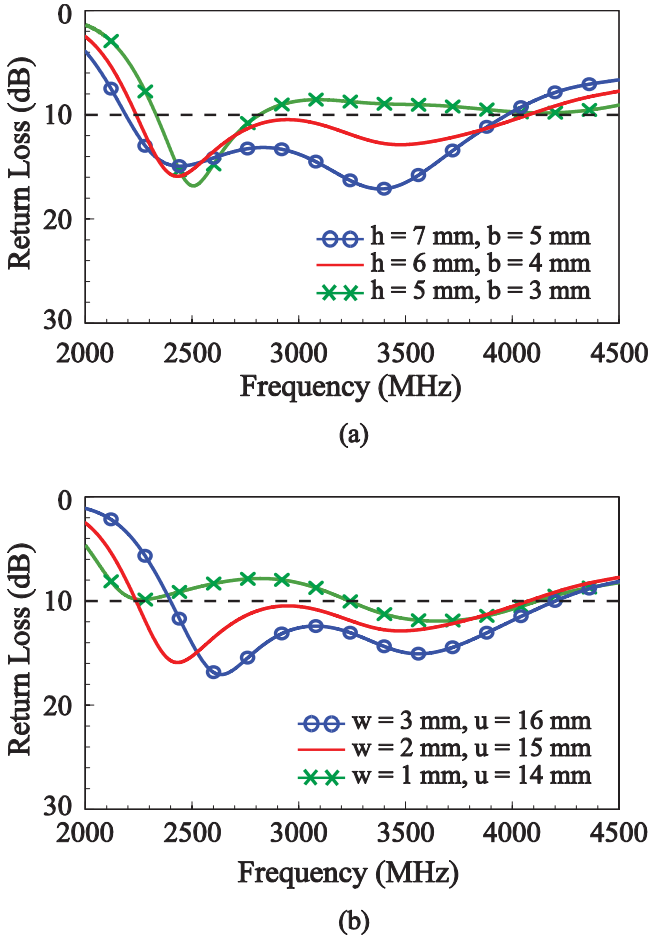

Figure 4 Simulated return loss as a function of (a) the height h and (b) the length w of the proposed antenna. [Color figure can be viewed in the online issue, which is available at www.interscience.wiley.com]

Effects of the width t and the angle α of the on-board slotted portion are studied in Figure 5. The results for the width t varied from 0 to 3 mm are shown in Figure 5(a). With an increase in t, the effective slot width is increased, and a widened bandwidth can be obtained. In this study, when the width t is chosen to be 3 mm, the obtained bandwidth is large enough for covering the desired WLAN/WiMAX operation. For the angle α, the results varied from 0° to 75° are shown. By selecting a larger angle, the impedance matching of the high-frequency portion of the antenna's operating band can be effectively enhanced. In this study, it is selected to be 45°, which is good enough for achieving a wide operating band to cover the desired WLAN/WiMAX operation.

Figure 6 shows the simulated return loss as a function of the slot length a. Note that the total length u of the antenna increases as the slot length a increases. It is clearly seen that the lower edge frequency of the operating band is effectively decreased with an increase in the slot length a. Effects of the slot width g on the add-on portion are studied in Figure 7, and results for the width g varied from 1 to 3 mm are presented. In this case, the height h of the add-on portion is fixed as 6 mm, and hence, the width g of the matching ground is varied as 6 mm − g in Figure 7. The lower edge frequency is not affected by the variations in the width g. However, it is important to select a proper width g (2 mm here) to achieve good impedance matching for frequencies over the desired operating band for WLAN/WiMAX operation.

Figure 8 shows the effects of the tuning-stub length c and the location d of the microstrip feedline. The results for the length c

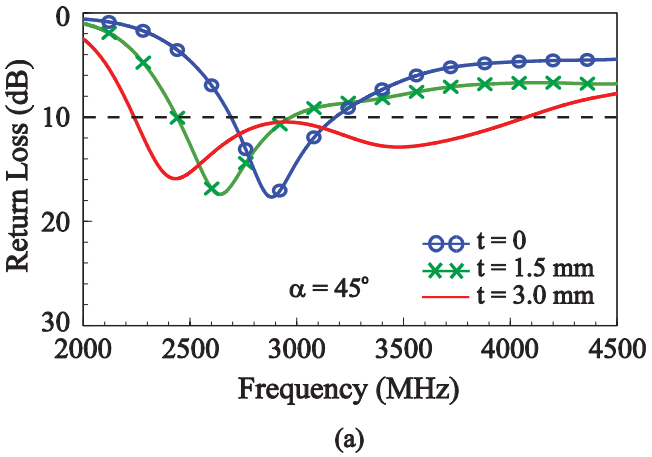

Figure 5 Simulated return loss as a function of (a) the width t and (b) the angle α of the on-board slotted portion of the proposed antenna. [Color figure can be viewed in the online issue, which is available at www.interscience.wiley.com]

varied from 0 to 5 mm are presented in Figure 8(a). Large effects of the length c on the impedance matching over the entire desired operating band are seen. The results for the location d varied from 0 to 2 mm are presented in Figure 8(b), and similar behavior as in Figure 8(a) is seen. The results suggest that the two parameters

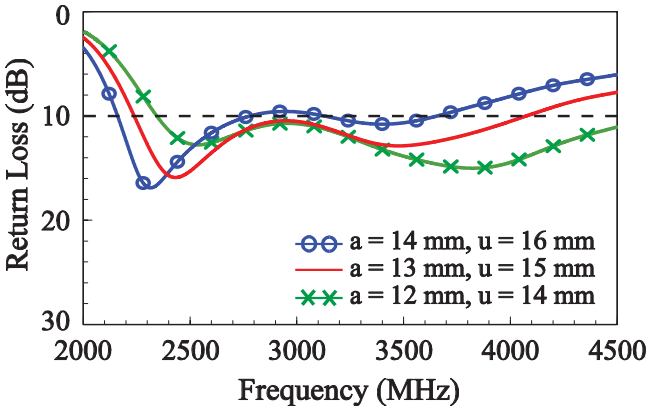

Figure 6 Simulated return loss as a function of the slot length a of the proposed antenna. [Color figure can be viewed in the online issue, which is available at www.interscience.wiley.com]

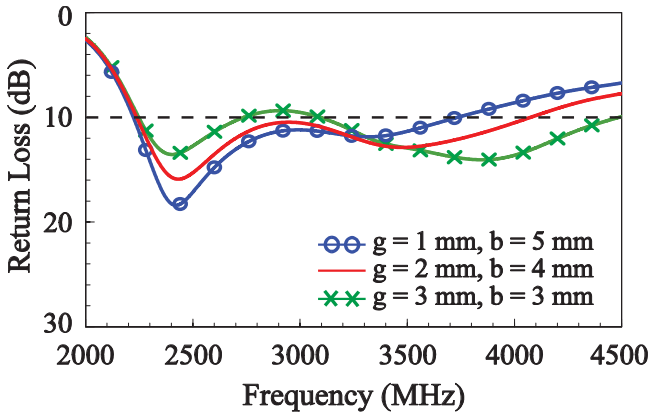

Figure 7 Simulated return loss as a function of the width g of the slotted region on the added-on portion. [Color figure can be viewed in the online issue, which is available at www.interscience.wiley.com]

related to the microstrip feedline are important for achieving good impedance matching over the desired operating band for WLAN/WiMAX operation.

Figures 9 and 10 plot the measured radiation patterns at 2500 and 3500 MHz for the proposed antenna. For both frequencies, comparable E_θ and E_ϕ components are seen in the x-y plane

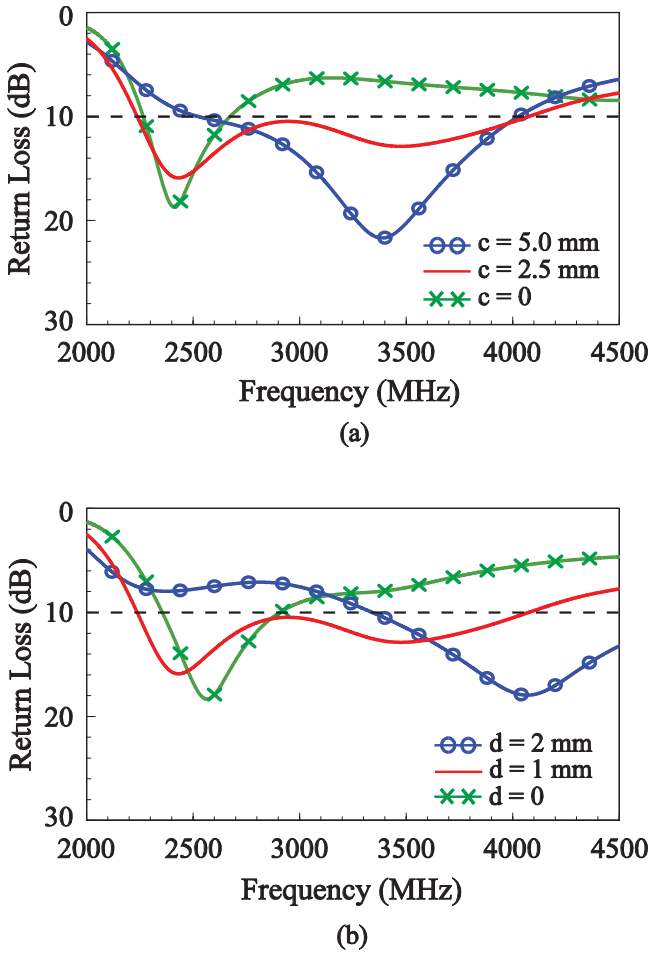

Figure 8 Simulated return loss as a function of (a) the tuning-stub length c and (b) the location d of the microstrip feedline. [Color figure can be viewed in the online issue, which is available at www.interscience.wiley.com]

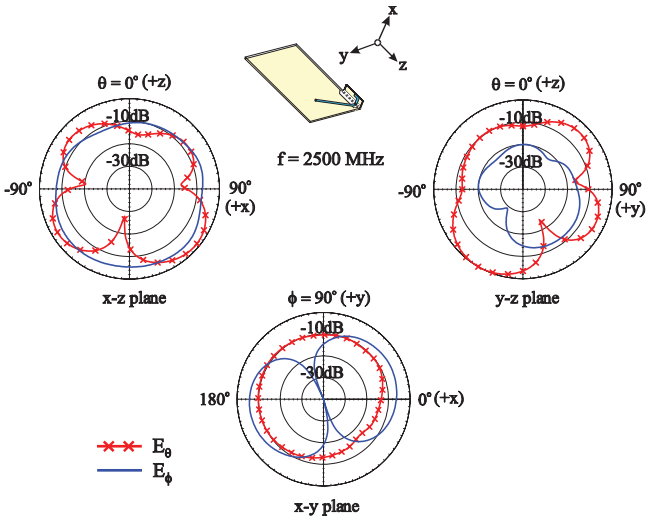

Figure 9 Measured radiation patterns at 2500 MHz for the proposed antenna. [Color figure can be viewed in the online issue, which is available at www.interscience.wiley.com]

(azimuthal plane). This is advantageous for practical applications since the wave propagation is usually complex for WLAN and WiMAX operation. For the two elevation planes (*x-z* and *y-z* planes), there are not much differences in the obtained radiation patterns for the two frequencies. The radiation patterns at other frequencies are also studied, and in general, there are no special distinctions in the radiation patterns for frequencies over the desired operating band. Figure 11 presents the measured antenna gain and simulated radiation efficiency for the proposed antenna. Over the operating band, the radiation efficiency is all larger than 80%. For the antenna gain, it is about 3.0–3.4 dBi over the 2.4 GHz WLAN band. Over the 2.5 GHz WiMAX band, the antenna gain is about 3.0–3.6 dBi, while over the 3.5 GHz WiMAX band, it is varied from about 3.5 to 4.2 dBi.

4. CONCLUSION

A novel wideband integrated monopole slot antenna suitable for mobile phone application has been proposed. The integrated

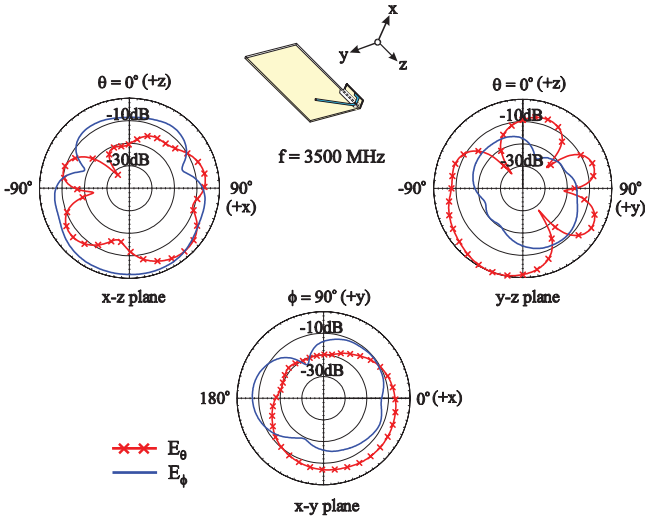

Figure 10 Measured radiation patterns at 3500 MHz for the proposed antenna. [Color figure can be viewed in the online issue, which is available at www.interscience.wiley.com]

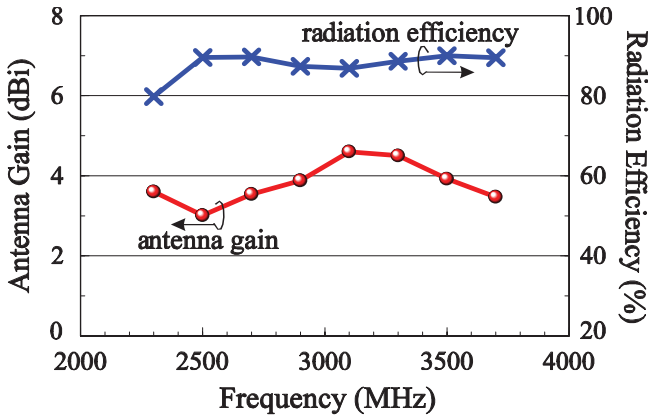

Figure 11 Measured antenna gain and simulated radiation efficiency for the proposed antenna. [Color figure can be viewed in the online issue, which is available at www.interscience.wiley.com]

monopole slot antenna is formed by mounting an add-on surface-mount portion to the system circuit board of the mobile phone and hence occupies a small area on the system circuit board. Yet, the proposed antenna generates a wide operating band of larger than 58% in 10-dB return-loss bandwidth, allowing it to easily cover WLAN operation in the 2.4 GHz band and WiMAX operation in the 2.5/3.5 GHz bands. Good radiation characteristics for frequencies over the obtained wide operating band have also been obtained. A parametric study on the dimensions of the proposed monopole slot antenna has also been presented. The proposed antenna also shows a small height of 6 mm only, which makes it promising for thin mobile phone applications.

REFERENCES

1. Worldwide interoperability for microwave access forum or WiMAX forum. Available at: http://www.wimaxforum.org.
2. Deployment considerations for fixed wireless access in 2.5 GHz and 3.5 GHz license bands, WiMAX Forum. Available at: http://www.wimaxforum.org/news/downloads/ DeploymentConsiderations_White_PaperRev_1_4.pdf, 2005.
3. K.L. Wong and L.C. Chou, Internal composite monopole antenna for WLAN/WiMAX operation for laptop computer, Microwave Opt Technol Lett 48 (2006), 868–871.
4. C.I. Lin, K.L. Wong, and S.H. Yeh, Wideband EMC chip antenna for WLAN/WiMAX operation in the sliding mobile phone, Microwave Opt Technol Lett 48 (2006), 1362–1366.
5. S.W. Su and K.L. Wong, Wideband antenna integrated in a system in package for WLAN/WiMAX operation in a mobile device, Microwave Opt Technol Lett 48 (2006), 2048–2053.
6. S.K. Sharma, L. Shafai, and N. Jacob, Investigation of wide-band microstrip slot antenna, IEEE Trans Antennas Propag 52 (2004), 865–872.
7. S.L. Latif, L. Shafai, and S.K. Sharma, Bandwidth enhancement and size reduction of microstrip slot antenna, IEEE Trans Antennas Propag 53 (2005), 994–1002.
8. A.P. Zhao and J. Rahola, Quarter-wavelength wideband slot antenna for 3-5 GHz mobile applications, IEEE Antennas Wireless Propag Lett 4 (2005), 421–424.
9. W.S.P. Lindberg, E. Ojefors, and A. Rydberg, Wideband slot antenna for low-profile hand-held terminal applications, Proc 36th European Microwave Conf. (EuMC2006), Manchester, UK, 2006, pp. 1698–1701.
10. R. Bancroft, Dual slot radiating single feedpoint printed circuit board antenna, U.S. Patent No. 7,129,902 B2, October 31, 2006.
11. W.S. Chen and K.Y. Ku, Broadband design of a small non-symmetric ground λ/4 open slot antenna, Microwave J 50 (2007), 110–120.
12. C.I. Lin and K.L. Wong, Printed monopole slot antenna for internal

multiband mobile phone antenna, IEEE Trans Antennas Propag 55 (2007), 3690–3697.
13. C.M. Su, H.T. Chen, F.S. Chang, and K.L. Wong, Dual-band slot antenna for 2.4/5.2 GHz WLAN operation, Microwave Opt Technol Lett 35 (2002), 306–308.
14. C.M. Su, H.T. Chen, and K.L. Wong, Inverted-L slot antenna for WLAN operation, Microwave Opt Technol Lett 37 (2003), 315–316.
15. K.L. Wong, Y.W. Chi, and S.Y. Tu, Internal multiband printed folded slot antenna for mobile phone application, Microwave Opt Technol Lett 49 (2007), 1833–1837.
16. K.L. Wong, Planar antennas for wireless communications, Wiley, New York, 2003.
17. Ansoft Corporation HFSS. Available at: http://www.ansoft.com/products/hf/hfss/.
18. K.L. Wong, L.C. Chou, and C.M. Su, Dual-band flat-plate antenna with a shorted parasitic element for laptop applications, IEEE Trans Antennas Propag 53 (2005), 539–544.

CHARACTERIZATION OF MULTIMODE FIBERS FOR USE IN MILLIMETER WAVE RADIO-OVER-FIBER SYSTEMS

Bilal A. Khawaja and Martin J. Cryan
Department of Electrical and Electronic Engineering, University of Bristol, Bristol, United Kingdom; Corresponding author: m.cryan@bristol.ac.uk

Received 13 December 2007

ABSTRACT: *Millimeter wave radio-over-fiber links using both single mode and, for what is believed to be the first time, multimode fibers are demonstrated over a 0–50 GHz bandwidth using a external Mach-Zehnder modulator operating at 1550 nm. The multimode fiber links show the potential for use in low-cost distributed antenna systems.* © 2008 Wiley Periodicals, Inc. Microwave Opt Technol Lett 50: 2005–2007, 2008; Published online in Wiley InterScience (www.interscience.wiley.com). DOI 10.1002/mop.23594

Key words: *millimeter wave; radio-over-fiber; Mach-Zehnder modulator*

1. INTRODUCTION

The demand for high-speed communication is increasing exponentially, and during the past few years, the idea of high speed in-building/campus wide radio-over-fiber (RoF) links at millimeter-wave (mm-wave) frequency bands have attracted much attention [1]. The mm-wave frequency bands are becoming attractive because at higher frequencies ($>$ 30GHz) and especially at 60 GHz they offer large transmission bandwidths and also overcome the problem of spectral congestion at lower frequency ranges [2]. In addition, mm-wave radio systems enable efficient frequency reuse because of the limited propagation distances at these frequencies. The 60-GHz band has a specific attenuation characteristic caused by water molecules (rain) and oxygen in the atmosphere (10–15 dB/km at 60 GHz) [2], which means for long-distance ($>$2 km) links many small closely spaced cells with small antennas will be necessary. Coaxial cables also become very lossy at 60 GHz and thus optical fiber becomes attractive and is emerging as an ideal medium for the distribution of mm-wave signals due to its low loss, low cost, large bandwidth, and immunity to electromagnetic interference characteristics.

For future high data transfer rate multimedia and VoIP-based applications, mm-wave RoF-links are considered to be a very good solution and they typically use single-mode fiber (SMF). RoF systems have already been demonstrated and tested in the 60-GHz frequency band using 20 km of SMF [3] and 37-GHz frequency bands using 50 km of SMF [4, 5]. There are both commercial as well as military applications of this technology. Commercial applications include broad-band signal distribution of interactive multimedia services to the home [4, 5] and personal radio communication [6]. Examples of military application are Doppler radar and phased array antennas [7]. SMFs are usually selected for long distance and high data rate RoF transmission systems but it is also desirable to utilize the existing fiber infrastructure to minimize the fiber installation and maintenance costs. However, the majority of the buildings in the United States and Europe already employ legacy links of 62.5-μm multimode fibers (MMF) with typical link lengths of 300–500 m, this MMF normally has a bandwidth as low as 160 MHz/km at a wavelength of 850 nm [8]. If this MMF fiber base could be reused for the transmission of mm-wave RoF links, it could save huge fiber installation costs enabling a new generation of mm-wave communication systems to be developed.

There has been much work carried out on extending the usable bandwidth of MMF [8, 9]. It was found [9] that even though the baseband bandwidth of MMF is limited to 500 MHz/km for a wavelength of 1310 nm, there are flat passband regions that extend into the microwave region. This occurs when a particular subset of modes are excited by the launch condition. The interference of these modes at the receiver will produce regions of high transmission which, with the use of mixers and local oscillators, can be used for transmission of baseband data. Thus, MMF has been used at much higher data rates and frequencies than had been thought possible. Recently, results have been shown as high as 25 GHz [10]. It is interesting to postulate what is the maximum frequency to which these passbands extend. This article seeks to extend the measurement region into the mm-wave band and results show good transmission properties to 50 GHz.

This article demonstrates a mm-wave RoF link up to 50 GHz using a 40-Gb/s external optical intensity Mach Zehnder-Modulator (MZM) with a 1550-nm tuneable laser light source over different lengths of SMFs and MMFs for future in-building/campus wide links. First, a SMF-based RoF link is presented and the chromatic dispersion problem that limits the link length is discussed, then results are shown for MMF-based RoF links.

2. SMF-BASED RoF LINKS

SMFs are normally used as the transmission medium for long haul systems and mm-wave RoF systems using SMF at the frequency ranges of 37–60 GHz [3–5] have already been demonstrated. In SMF, signal-quality degradation is usually negligible for ($<$1 km) links. Although dispersion-induced RF-signal fading is not a problem at low radio frequencies, it does become problematic when operating in mm-wave frequency bands [11]. Gliese et al. [11] show that in standard SMF the dispersion of 17 ps/(nm km) at 1550 nm wavelength causes time lag between the modulation sidebands, and at 60 GHz a 1-dB penalty was induced after 500 m of standard SMF. Beyond 1 km the dispersion problem can become so severe that the original signal can be completely cancelled out. Smith and coworkers [12] proposed two solutions for overcoming the chromatic dispersion in SMF-based links using external modulators. The first method was to increase the link distance by varying the MZM chirp parameter and the second method uses a single sideband (SSB) modulation technique by implementing a dual-electrode MZM. Externally modulated or directly modulated mode-locked lasers (MLLs) may also overcome the dispersion problem [4].